Zero-bias anomaly in homogeneously disordered MoGe nanowires undergoing a superconductor-insulator transition

Hyunjeong Kim and A. Rogachev

Phys. Rev. B **94**, 245436 — Published 28 December 2016

DOI: 10.1103/PhysRevB.94.245436

Zero-bias anomaly in homogeneously disordered MoGe nanowires undergoing a superconductor-insulator transition

Hyunjeong Kim and A. Rogachev

Department of Physics and Astronomy, University of Utah
Salt Lake City, 84112, Utah, USA.

Abstract

Nanowires made of superconducting Mo-Ge alloys undergo a superconductor-insulator transition when their cross sectional area is reduced. On the insulating side of the transition, the differential resistance of the nanowires drops with voltage and displays a positive zero-bias anomaly (ZBA). To reveal the origin of this ZBA, we fabricated and studied a series of nanowires made of amorphous alloys with composition $Mo_{50}Ge_{50}$. The length of wires was in the range 150 nm – 11 μm and width in the range 10-20 nm. We also fabricated and measured several more complex nanowire-based structures: (i) a nanowire gated by a nearby film electrode, (ii) a nanowire connected to film electrodes with an "adiabatically reduced" width, (iii) a nanowire with a multi-electrode configuration which allowed comparison of different sections of the same nanowire, and (iv) a nanowire with different sizes of film electrodes. We found that for $Mo_{50}Ge_{50}$ nanowires all experimental parameters of the ZBA and their dependence on nanowire length can be explained by electron heating. Several physical processes thought to be responsible for the ZBA have been analyzed and rejected.

1. Introduction

It is now well established that a discontinuous superconductor-insulator transition (SIT) takes place in several disordered two-dimensional superconducting film systems[1,2,3,4,5,6]. Rather unexpectedly, recent experiments indicate that a direct SIT can also occur in long *one-dimensional* superconducting nanowires[7,8]. It was found that this transition can be driven by a magnetic field, nanowire cross sectional area, and possibly by aspect ratio of a nanowire cross section. The nature of the SIT in nanowires is not understood. Moreover, many other experiments on superconducting nanowires revealed a gradual crossover from superconducting to metallic state rather than a direct SIT [9,10,11,12,13]. The crossover behavior, which experimentally appears as a flattening of $R(T)$ curves at the lowest temperatures, is believed to be caused by quantum phase slips (QPS), topological fluctuations of the order parameter [14,15]. Alternatively, the flattening could also be related to artefacts of the experiments, such as the granularity of the nanowires and improper noise filtering.

In superconducting films close to the critical point, the low-bias resistance isotherms follow the finite size scaling model[4,5,16,17], which gives strong indication that the SIT in films is also a quantum phase transition (QPT). In addition, it has been shown that in amorphous MoGe [5] and NbN [17] films, *nonlinear* differential resistance measured as a function of magnetic field at several finite bias voltages also scales both on the insulating and superconducting sides of the SIT. The combined analysis of temperature and electrical field scaling had a great advantage, since it allowed separate determination of the correlation length exponent ν and dynamical exponent z. However, an extension of this analysis to another classical system displaying an SIT, quench-condensed amorphous Bi films, was not successful. In fact, it was concluded that non-linear resistance on the insulating side comes from an electron heating effect [18] and overall validity of the combined analysis was questioned.

Similar to MoGe films, long MoGe nanowires display nonlinear behavior, which appears experimentally as a zero bias anomaly (ZBA) in differential resistance, dV/dI. Exactly as in the case of MoGe films, the ZBA in nanowires changes sign from negative to positive at the critical point of the SIT[7]. On the superconducting side, the non-linear behavior is likely related to the critical superconducting current in nanowires; the origin of the ZBA on the insulating side is not understood and is a focus of the present paper. Overall evolution of linear and non-linear resistance in MoGe nanowires suggests the presence of a quantum phase transition of yet-unknown nature. Understanding the origin of the ZBA

could help to decide if non-linear resistance can be incorporated into the scaling analysis of QPT, as well as help to resolve the issue with non-linear resistance in films.

In general, the ZBA is not a unique experimental feature and can be caused by of various physical phenomena. Examples include the effect of electron-electron interaction on tunneling conductance in disordered metals[19], a Luttinger liquid[20], the Kondo effect in quantum dots[21], the two-channel Kondo effect[22,23], an environmental Coulomb blockade[24,25], and several others. The distinction between different mechanisms is not straightforward and is often obtained from the detailed analysis of voltage and temperature dependences of the ZBA and/or an observation of a scaling relation for $G(T,V)$ curves. To reveal the origin of the ZBA in nanowires, we carried out low-temperature transport measurements on MoGe nanowires spanning the length from 150 nm to 11 μm. In contrast to previous studies[26,27,28,29,30], we used the advantage of our fabrication method, high-resolution electron-beam lithography, and fabricated and studied several nanowire-based structures with varying size and geometries of electrodes and with a side gate. We have not found any change in the ZBA parameters in these more complex nanowire-based devices; this allowed us to consider and reject several physical processes thought to be responsible for ZBA.

2. Characterization of nanowires: Electronic parameters of Mo-Ge alloys.

We studied the low-temperature transport properties of more than 20 MoGe nanowires located on the insulating side of the superconductor-insulator transition. These nanowires were fabricated using negative electron beam lithography with hydrogen silsesquioxane (HSQ) electron-beam lithography resist; the details of the fabrication are given in the Supplementary Materials to Ref. [7]. In our fabrication procedure, a nanowire is smoothly connected to rectangular film electrodes, which are made from the same original MoGe film. Voltage and current leads are connected to the opposite sides of the electrodes; we refer to this connection as the quasi-4-probe geometry. In our precious work we fabricated several nanowires in true-4-probe geometry, where nanowires served as the voltage probes[7]. No difference between two methods was found. The fabricated nanowires had a rectangular cross section with thickness 4-5 nm and width 10-20 nm; the length of the wires, L, was in the range 150 nm – 11 μm. MoGe alloy has an amorphous atomic structure; the mean free path in these material is close to the interatomic distance. As a result, the bulk resistivity, ρ_v, at room temperature (where quantum corrections can be neglected) does not depend on size of the nanowire. The cross sectional area, A, of a nanowire can be estimated from room temperature resistance, R_0, as $A = \rho_v L / R_0$. Alternatively, a wire may be characterized by the resistance per length defined as $\rho_L = R_0 / L$. We studied a series of samples with relative Mo-Ge content $Mo_{50}Ge_{50}$ ($\rho_v = 235$ μΩ cm). Transport measurements were carried out in a He-3 cryostat equipped with well-filtered leads. The design of the filters is described in the Supplementary Materials to Ref. [7].

For the analysis of the data presented in the body of the paper, we need to summarize and estimate some physical parameters of the alloy. To estimate the density of amorphous a-$Mo_{50}Ge_{50}$ alloy we first estimated the density of hypothetical crystalline $Mo_{50}Ge_{50}$ compound by an extrapolation between the densities of two intermetallic compounds Mo_5Ge_3 ($\rho_c = 9.63\,\mathrm{g/cm^3}$ [31]) and $MoGe_2$ ($\rho_c = 8.83\,\mathrm{g/cm^3}$ [31]) and then multiplied it by the factor 0.86=0.64/0.74 (the ratio of filling factors for randomly and closely-packed spheres); this gives $\rho_a = 8.0$ g/cm^3. The estimated electron specific heat coefficient γ is 2.32 mJ/moleK^2 (extrapolated between two neighboring data points)[32]. We estimate the electronic specific heat per unit volume, $\gamma_V = 2.2\times10^2$ J/m^{3}K^2, using ρ_a and γ. The density of states at the Fermi level, $g(0)$, was then obtained using relation $\gamma_V = \pi^2 k_B^2 g(0)/3$. We thus find value 3.50×10^{47} J^{-1}m^{-3} (5.6×10^{22} eV^{-1}cm^{-3}) for a-$Mo_{50}Ge_{50}$. These estimates ignore possible electron-phonon enhancement of γ by the factor of 1.1-2 [33]. To proceed further, we assume the Fermi surface of the alloys is spherical, but because of the presence of a d-element the effective mass of carriers, m^*, is not equal to the free electron mass m_e; this is fairly standard starting approximation for amorphous or liquid metals [34]. We also

assume following Ref. [35] that the mean free path is equal to interatomic distance $l \approx 0.3$ nm. This is just a good guess; unfortunately because of the unknown m^*, l can't be determined accurately. The choice of l is supported by the experimentally determined value of $l \approx 0.43$ nm in amorphous $Ag_{40}Cu_{40}Ge_{20}$ alloy, which, according to Hall and specific heat measurements, follows accurately the free electron model with the electron density consistent with one free electron provided by each Ag and Cu atom and four electrons by Ge[36]. A somewhat smaller value of l is expected in an amorphous alloy with d-electrons. Taking $l \approx 0.3$ nm and using the free electron model relations $\sigma = e^2 n\tau / m^* = e^2 l k_F^2 / 3\pi^2 \hbar = e^2 Dg(0)$ we find: Fermi wave vector $k_F = 1.3\times10^{10}\,\mathrm{m}^{-1}$, density of carriers $n = 0.76\times10^{29}\,\mathrm{m}^{-3}$, diffusion coefficient $D = 4.7\times10^{-5}\,\mathrm{m}^2/\mathrm{s}$, elastic scattering time $\tau = 6.4\times10^{-16}\,\mathrm{s}$, and $m^* = 3.2m_e$.

3. Long nanowires. Results and discussion.

Fig. 1a shows the low-bias resistance versus temperature for three representative nanowires, which are labeled as K1, K2 (length of both wires is 3 μm) and I1 (length 2.3 μm). The data are normalized by the value of resistance at $T = 4$ K, R_{4K}. The figure indicates the resistance per length at 4 K for each wire. At temperatures higher than 4 K, the nanowires' resistance changes weakly and typically drops by a few percent between 4 K and 300 K. Below 2 K, as the figure shows, the data can be well fitted by the equation $R(T)/R_{4K} = B + \alpha T^{-\beta}$. The shown fitting curves were obtained with fixed $\beta = 0.5$; this power corresponds to a quantum correction due to the electron-electron interaction (EEI)[19]. We performed the fitting for all the wires using the above equation, letting β be a free parameter. We found that values appear in the range 0.3-0.5 and show a rough tendency of increasing β with decreasing nanowire cross-sectional area. The likely reason is that the width of our thickest wires are comparable to the thermal length $L_T = \left(\hbar D / k_B T\right)^{1/2}$ (for $T = 1$ K, $L_T \approx 20$ nm) and they are not strictly in one-dimensional regime.

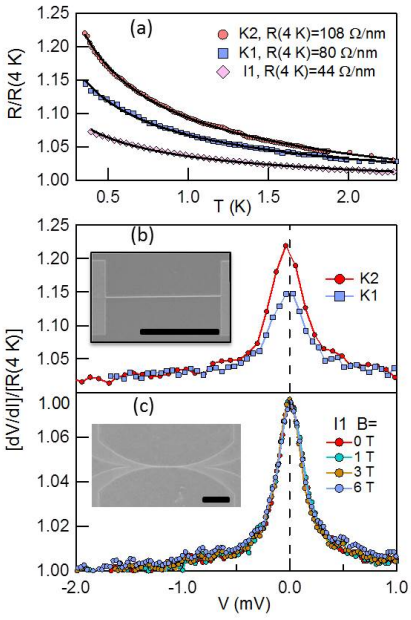

Fig. 1. (a) Resistance versus temperature for three $Mo_{50}Ge_{50}$ nanowires in zero magnetic field. The length of nanowires K1 and K2 is 3 μm, the length of I1 2.3 μm. (b) Differential resistance as a function of voltage at T=0.3 K for K1 and K2 nanowires. The inset shows the scanning electron microscopy (SEM) image of nanowire K1 fabricated with rectangular film electrodes. (c) Differential resistance as function of voltage at T=0.35 K for nanowire I1 at indicated magnetic fields. The inset shows the SEM image of the nanowire I1 smoothly connected to "adiabatic" film electrodes. The length of the scale bars in both insets is 2 μm.

The measured differential resistance, dV/dI, normalized by R_{4K}, is plotted as a function of voltage for nanowires K1, K2, and I1 in Fig.1b and Fig.1c. This variation is strongly non-linear and reveals a zero bias anomaly with a sample-dependent characteristic width of a fraction of a mV at $T = 0.35\,\mathrm{K}$. Comparing these data with $R(T)$ dependences, one can notice that the height of the ZBA is approximately equal to the gain of the low-bias resistance between 4 K and 0.3 K.

In the Fig. 2, we show the non-linear differential conductance (the inverse of the dV/dI) for the nanowire I1, measured at the indicated temperatures. One can see that with increasing temperatures, the anomaly gets broader. Also, above a certain voltage, the conductance becomes temperature-independent and varies, as the fitting curve shows, as $G = G_0 - \gamma V^{-0.5}$. This approximation also works well in the high-bias regime of the other nanowires.

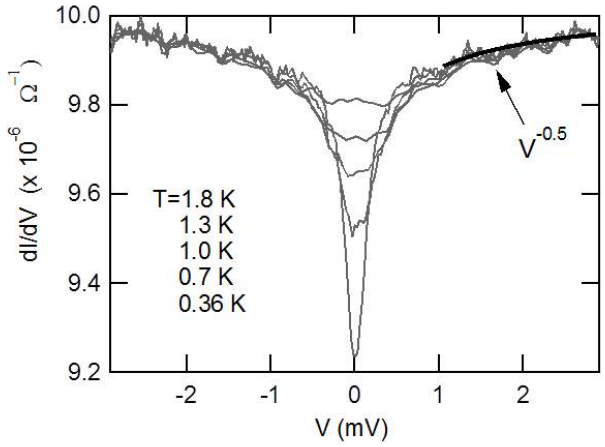

Figure 2. Differential conductance as a function of bias voltage for nanowire I1 at indicated temperatures between 0.36 and 1.8 K (from the bottom to top). The thick solid line indicated the T-independent $G = G_0 - \gamma V^{-0.5}$ *variation.*

Let us discuss (and reject) several possible mechanisms that could be responsible for the zero bias anomaly. A ZBA was theoretically predicted to appear in very long *superconducting* nanowires at low temperatures when quantum phase slips proliferate and destroy phase coherence in a wire[37]. More specifically, the anomaly occurs because of the formation of bound pairs of quantum phase slips with $+2\pi$ and -2π phase change; increasing current weakens the bonding in these phase-slip-antiphase-slip pairs and decreases the resistance of a wire, thus producing a ZBA in the differential resistance. To verify the presence of these processes, we made transport measurements of the nanowire I1 in various magnetic fields (Fig. 1c). The lack of any magnetic field dependence indicates that the origin of the ZBA in MoGe nanowires with weakly insulating behavior is not related to superconductivity, including the effects of QPS. The Kondo mechanism of the anomaly can be rejected on the same grounds. The lack of a magnetic field effect on conductance of disordered nanowires appears to be rather common and similar behavior has been observed in AuPd nanowires[38].

A zero bias anomaly in the *tunneling density of states* is a distinct feature of electron-electron interactions in disordered materials; the description of this phenomenon is given by the Altshuler-Aronov theory[19]. This theory was employed to explain the $V^{-1/2}$ variation of the conductance observed in Hg nanowires with diameters in the range 2.5-6 nm [29] (see also Ref. [19] p. 51) prepared by filling channels in chrysotil asbestos with Hg under pressure. In these experiments, the *resistance* across samples containing many Hg filaments was measured and in this regard, it is similar to our experiments. The authors excluded heating effects and suggested that the filaments are not continuous but have breaks and

thus the voltage dependence originates from the tunneling resistance of these breaks. We found no evidence for such breaks in our MoGe nanowires. The width of the MoGe wires, inspected with the scanning electron microscopy (SEM), was uniform and the resistance of the wires agreed well with simple formula $R_0 \approx \rho_v L / A$.

To further test the possible presence of segmentation in MoGe nanowires, we fabricated a device with a planar gate electrode placed at the distance of 500 nm from the nanowire. A study of very similar nanowire-based structures made of InO revealed the presence of hundreds of Coulomb blockade oscillations produced by varying gate voltage[39]. This behavior was taken as an evidence of the separation of a structurally continuous InO nanowire into several segments connected by tunneling junctions. In contrast to InO nanowires, we did not observe any Coulomb oscillations in the gated MoGe structure.

One may further argue that MoGe nanowires could have an "intrinsic" granularity related to the properties of material itself with spatial scale too small to be affected by the distanced gate. This is unlikely to be the case. Atomic structure of MoGe alloys with different relative content of Mo and Ge have been thoroughly studied via extended x-ray-absorption fine structure, differential anomalous scattering, and small-angle x-ray scattering[40]. The alloy relevant to the present study, $Mo_{50}Ge_{50}$, was shown to have uniform amorphous structure with no small-scale phase separation. (A separation into two amorphous phases with 2-4 nm length scale was detected only in Ge-rich alloys, $Mo_X Ge_{1-X}$ with $x < 0.23$, by anomalous small-angle X-ray scattering[41,42].) Our conditions for the deposition of MoGe alloy are very similar to that used for fabrication of the samples employed in structural studies and important parameters, such as resistivity and T_C, are well reproduced. We can therefore reject the possibility that the ZBA in MoGe nanowires is due to separation of the nanowires into segments connected by tunneling junctions or intrinsic granular atomic structure of the material.

Similarly to the Hg nanowires studied in Ref. [29], a zero bias anomaly has been observed in Ni nanowires (12-16 nm in diameter) fabricated by electrochemical deposition of Ni into parallel pores of anodic aluminum oxide[30]. However, in the latter case, the Ni nanowires were contacted from one side by anodized Al, which served as a high-resistive tunneling junction to the array. The ZBA observed in these Ni nanowires was explained with the theory of environmental Coulomb blockade[43,44]. The ratio of the tunneling resistance to the resistance of the wire was large, though this condition needs not be fulfilled for the observation of a Coulomb blockade[45]. The data for both Ni and MoGe nanowires look qualitatively similar, despite the fact that the geometries of the structures are distinct. The majority of our MoGe nanowires had the structure shown in the inset in Fig. 1b. In our fabrication procedure, the nanowires and rectangular electrodes are made from the same original MoGe film and go through the same steps of lithography and etching. Therefore, the formation of a structural discontinuity at the nanowire-electrode interface, which could serve as a tunneling junction, is unlikely. This assumption is supported by the fact that we didn't detect any extra interface resistance in slightly thicker superconducting MoGe nanowires fabricated by the same method[7]. The picture, however, can be more complicated since recent theories suggest that a tunneling junction, in fact, is not needed for observation of a Coulomb blockade; any coherent scatterer can serve as an "effective" tunneling junction [46,47]. In particular, even in the absence of morphological or structural defects, coherent scattering can occur at the nanowire – rectangular electrode connection because of the discontinuity in the number of quantum channels. This was one of the arguments to suggest coherent-scatterer Coulomb blockade as the origin of the ZBA in very short (50-150 nm) MoGe nanowires[26]. To verify this possibility, we fabricated and tested several wires with electrodes gradually narrowing to nanowire width. The SEM image of one of the samples (I1) with such "adiabatic" electrodes is shown in the inset to Fig. 1c. The structure mimics the connection used in co-planar microwave circuitry to eliminate impedance mismatch and is expected to remove or diminish the effective barrier. We did not find any difference in behavior of the nanowires with "adiabatic" and rectangular electrodes. We therefore conclude that the Coulomb blockade as the origin of the ZBA in long nanowires can be dismissed.

To further clarify whether the ZBA in nanowires is produced by a local process or related to the global parameters of a nanowire, such as length or total resistance, we fabricated and studied a three-

electrode device, nanowire U3, schematically shown in the right inset of Fig. 3. In this device, in addition to the standard rectangular four-electrode configuration (labeled A,B,C,D in the figure) we added a fifth nanowire electrode, E, which had the same width as the main nanowire and divided it into two parts. With electrodes A and C serving as current leads, the device allowed for measurements of three sections of the main nanowire with length 3, 6 and 9 μm. The device was made in a single run of e-beam lithography from the same MoGe film. All the sections of the nanowire had the same width and thickness, which allowed combined scaling analysis of three sets of data. (This could not be done on separately fabricated wires.)

We varied the electrical current and measured differential resistance and voltage across each section. Analyses showed that the data for three sections fall on the same curve if plotted as resistance per length, $\rho_L = R/L$, versus electrical field, $E = V/L$ across each section. We observed an excellent collapse of the data both at high electrical fields, as shown in the main panel of Fig. 3, and at low fields, as shown in the left inset. The experiments clearly demonstrate that, at least in sufficiently long nanowires, the ZBA is caused by local processes.

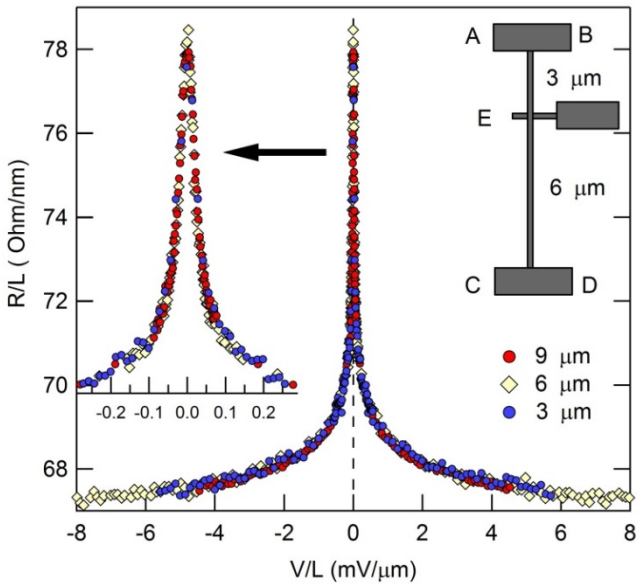

Figure 3. Differential resistance per unit length versus voltage per length for a three-terminal nanowire U3 at T=0.3 K. Independently measured data across three sections with length 3,6, and 9 μm are superimposed and fall one on top of the other. The left inset zooms in the low-bias range. The right inset sketches the geometry of the sample. (Terminals A and C serves as the current leads and B, E, and D as the voltage leads)

In the next step of the analysis, we compiled the data from our standard samples with rectangular electrodes (geometry shown in the inset to Fig 1b) and proceeded as follows. For each nanowire, the dV/dI versus V dependence at the lowest temperature of measurements (range 0.3-0.4 K) was fitted at high voltages with the dependence $R(V) = R_0 + a/\sqrt{V}$, where R_0 and a were the fitting parameters. R_0 determines the base of zero bias anomaly. Using R_0, we extracted two parameters characterizing the ZBA: the relative height of the anomaly, $h_A = (R(V=0) - R_0)/R_0$, and the width of the anomaly, w_A, at $0.5h_A$. In Fig. 4a, we plot h_A versus resistance per length R_0/L. This dependence is approximately linear, as expected from the theory of quantum corrections[19]. Interestingly, the three shortest studied nanowires (with length 150 nm) follow the same dependence, indicating that the magnitude of the correction does not depend on the wire length. Our observation differs from the data for AuPd nanowires

where the quantum correction was found to decrease strongly for wires with length smaller than 5 μm [48,49]. The disagreement is surprising, since two materials have close resistivity ($\rho_v = 375\ \mu\Omega\ \mathrm{cm}$ for AuPd [42]). On the other hand, the lack of any length dependence of h_A on length in MoGe nanowires is expected from the theory [19,43] as the change of regime is set by the thermal length, $L_T = (\hbar D / kT)^{1/2}$, which for MoGe at $T = 0.3\ \mathrm{K}$ is $L_T \approx 40\ \mathrm{nm}$, smaller than the length of shortest studied wires.

In Fig. 4b we plot the mid-height width of the zero bias anomaly divided by nanowire length, w_A / L, as a function of the length of nanowires. These data indicate the presence of two regimes, above and below $L \approx 2\ \mu\mathrm{m}$. The parameter w_A / L quantifies the electrical field, needed to decrease the height of anomaly by a factor of 2. Because this parameter is roughly constant in nanowires with length above $2\ \mu\mathrm{m}$, we conclude that in these nanowires, the ZBA is controlled by the electrical field. This is consistent with the behavior of the three-electrode structure described above and overall indicates that in long nanowires, the ZBA is caused by local processes.

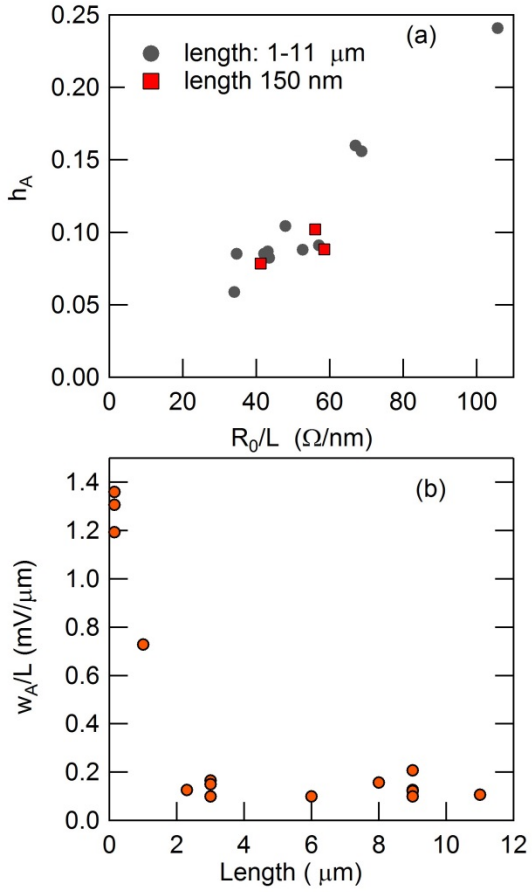

Figure 4. Parameters of zero bias anomaly at the lowest temperature of measurements (0.3-0.4K). (a) Relative height of the anomaly versus linear resistivity. (b) The width of the ZBA over nanowire length versus length of a nanowire.

The most natural candidate for a local process causing the ZBA is electron heating. Via this mechanism, an electron moves in an electrical field and experiences many random elastic collisions; work done by the electrical field increases its kinetic energy, which is eventually transferred to the lattice when

electron-phonon scattering takes place. As a result, the effective temperature of the electrons can be larger than that of the lattice and, if the resistance is temperature-dependent, the effect of the electrical field is roughly equivalent to an increase in temperature. To evaluate this effect quantitatively, one needs to know the characteristic electron-phonon scattering time, τ_{ep}. Unfortunately for Mo-Ge alloys, we know τ_{ep} only from a single source, a measurement of the magnetic field dependence of the quantum correction to conductivity for 3.6-nm-thick *a*-$Mo_{78}Ge_{22}$ film in the temperature range 7-16 K[35]. The temperature dependence τ_{ep} : $1/T^2$ observed in these experiments appears to be fairly common in disordered films and, in some cases, was found to extend down to 0.3-1.5 K [50]. Extrapolating the data of Ref. [35], we get an estimate $\tau_{ep} \approx 1.6\times10^{-8}$ s at *T*=0.3 K.

The effective electron temperature can be found approximately from the relation [51]

$$\Delta T = T_e - T_{latt} = \tau_{ep}\sigma E^2 / \gamma_V T_{latt}. \quad (1)$$

Experimentally found electrical field at the mid-height of the ZBA is $E = 60$ V/m for nanowires K2 and I1 and $E = 50$ V/m for the three-terminal nanowire U3; the estimated effective electron temperature gain is $\Delta T \approx 400$ mK for K2 and I1 and $\Delta T \approx 250$ mK for U3. From the low-bias $R(T)$ dependence we find that the *T*-dependent correction drops to half at $T \approx 0.7$ K and $\Delta T \approx 0.4$ K. Hence we are led to conclude that, providing the estimate of τ_{ep} is accurate, the ZBA in long *a*-$Mo_{50}Ge_{50}$ nanowires is dominated by electron heating. This conclusion is supported by the fact that the electron-phonon scattering length estimated as $L_{ep} \approx (D\tau_{ep})^{1/2} \approx 900$ nm at 0.3 K is close to the boundary between the two regimes shown in Fig. 4b. Indeed, in nanowires with $L < L_{ep}$, an electron can escape to the electrodes between consequent electron-phonon collisions. As a result, the gain of kinetic energy decreases and a higher electrical field becomes necessary to reach the same effective electron temperature.

Let us also notice that the height of the anomaly does not depend on the electron heating *per se*. In fact, the anomaly occurs because the magnitude of the quantum corrections depends on *temperature*; as we mentioned above, the height of the ZBA is approximately equal to the change of the low-bias resistance between 4 and 0.3 K.

4. Short nanowires. Results and discussion.

The dependence of the ZBA width-over-length parameter on the length of nanowires, shown in Fig. 4b, clearly indicates that in nanowires with a length below 2 μm, a new mechanism of ZBA suppression becomes relevant. In this section, we analyze the behavior of our shortest 150-nm-long nanowires. They are significantly shorter than the electron-phonon scattering length, 900 nm, but longer than the thermal length, $L_T \approx 35$ nm (both at $T = 0.3$ K). Two other relevant lengths scales are the dephasing length, $L_\varphi = \sqrt{D\tau_\varphi}$, and electron-electron (e-e) scattering length, $L_{ee} = \sqrt{D\tau_{ee}}$. The time corresponding to the latter process can be found from the expression (Eq. 4.4 in Ref.[19]).

$$\frac{1}{\tau_{ee}} = \left\{1 - \frac{3F}{4+F}\left[1 - \left(1 + \frac{F}{2}\right)^{1/2}\right]\right\} \frac{1}{\sqrt{2}\pi\hbar g_1(0)} \left(\frac{k_B T}{\hbar D}\right)^{1/2}, \quad (2)$$

where $g_1(0) = g(0)A$ is the density of states per unit length of the wire and F is the parameter characterizing e-e interaction. It can be found from the formula $F = 2\ln(1+x^2)/x^2$, where $x = 2k_F / k_{TF}$ and $k_{TF} = (e^2 g(0)/\varepsilon_o)^{1/2}$ is the Thomas-Fermi wave vector. Using the parameters estimated in section 2, we find $F = 1.53$. For a wire with a typical cross-sectional area $A = 60$ nm^2 we estimate that at *T*=0.3 K $\tau_{ee} \approx 2.7\times10^{-10}$ s and $L_{ee} \approx 110$ nm. The theory claims that in disordered 1D wires at low temperature, the dephasing time is dominated by e-e scattering; the corresponding τ_φ can be found from the formula (Eq. 4.33 in Ref. [19])

$$\tau_\varphi = \left(\frac{\sigma A \mathrm{h}^2}{e^2 k_B T D^{1/2}} \right)^{2/3}. \qquad (3)$$

For a cross section area $A = 60$ nm^2 and T=0.3 K, we estimate $\tau_\varphi = 5.3 \times 10^{-11}$ s and $L_\varphi = 50$ nm for *a*-$Mo_{50}Ge_{50}$ nanowires.

The zero bias anomaly in *short a*-$Mo_{78}Ge_{22}$ nanowires was carefully studied in Ref. [26]. The nanowires were fabricated by deposition of material on top of suspended carbon nanotubes; the length was varied over a range of 40-150 nm. The results were then interpreted within the theory of Coulomb blockade (CB) in diffusive wires proposed by Nazarov [46]. This theory claimed that the CB can still be present in a geometry in which the plates of a capacitor are connected by a multi-channel disordered wire, provided the wire is short enough to behave as 0-dimensional coherent scatter. Golubev and Zaikin derived the $I(V)$ and $R(T)$ characteristics of this phenomenon[52]. It was found that in the high temperature regime ($k_B T > E_C$, where E_C is the charging energy of a capacitor), the predicted shape of the ZBA of a diffusive wire is very similar to that of a single tunneling junction[53,54,55]. In particular, in both cases the width of the anomaly at half-height was related to the temperature as $\Delta V_{1/2} \approx 5.44 k_B T / e$. The ZBA in *a*-$Mo_{78}Ge_{22}$ nanowires studied in Ref. [26] was found to follow these predictions. The theory [46,54] was also used to explain the behavior of the ZBA in Cu nano-bridges[27,28] (which have much a smaller resistance, $R = 5\ \Omega$). The interpretation based on Coulomb blockade has left unresolved an important question regarding the origin of the charging energy. It was assumed that the relevant capacitance is the one between coplanar electrodes; however, this has been proven neither for the short MoGe nanowires nor for the Cu bridges. Another problem with the CB interpretation is that MoGe nanowires were not exactly within the length restriction required by the theory, $L << L_{ee}, L_T, L_\varphi$.

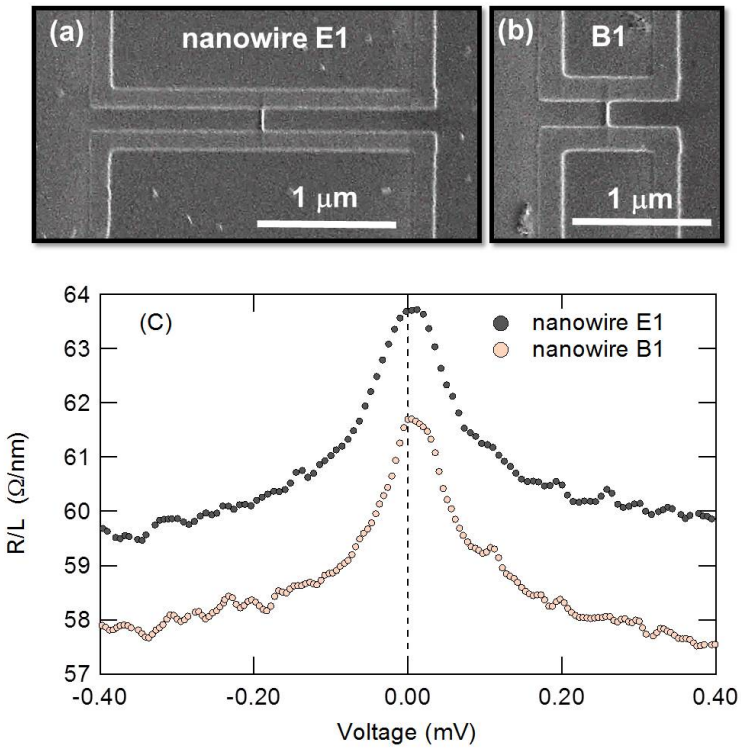

Fig. 5 (a) SEM image of nanowire E1 with the portion of the electrodes. (b) The same for nanowire B1. (c) Differential resistance over length versus voltage at temperature T=0.4 K for nanowires E1 and B1.

With these problems in mind, we fabricated and tested three nanowires with length 150 nm. Two of these nanowires, E1 and B1, had very close normal state resistance. Figure 5 shows SEM images of the nanowires and the dependence of their differential resistivity on voltage. Using the method described in the previous section, we determined the width of the anomaly at the mid-height and found that it relates to the temperature as $w_A = A_0 k_B T / e$ with an experimentally determined coefficient A_0 being 5.7 , 5.8 and 5.2 for nanowires E1, B1, and B3 (data are not shown), respectively. These results appear consistent with Ref.[26] and with the theoretically expected value $A_0 \approx 5.44$, seemingly confirming the interpretation based on the weak Coulomb blockade.

It was suggested in Ref. [26] that the capacitance responsible for the CB in the nanowires was the capacitance between two coplanar electrodes connected to it. This determines the relative height of the ZBA and depends linearly on the width of electrodes, but only logarithmically on their lateral extension away from the wire. It was also assumed that, similar to the case of a single tunneling junction, the portion of electrodes contributing to the CB is limited by a "horizon". To test the presence of the CB more directly, we fabricated nanowires E1 and B1 so that they had almost the same room temperature resistance but the width of the electrodes of nanowire E1 was three times that of B1. Figure 5(a,b) shows SEM images of these two structures. The measured ZBA for these nanowires is shown in Fig. 5(c) and it is clear that the height of the anomalies is essentially the same; the width of electrodes appears to be not important. This suggests that the CB is not the mechanism responsible for the anomaly. An additional argument against the CB interpretation comes from the data in Fig. 4(a), which shows that the height of the anomaly both in short and long wires is consistent with each other and is set by the linear resistivity of the nanowires. We notice that for short nanowires with length $L_\varphi < L$, Golubev and Zaikin developed another theory[56] which claims that the height of the anomaly is given by the same relation as in Ref. [54], $h_A = E_C / 9k_B T$, but the effective charging energy depends only on the parameters of nanowires, $E_C = 3/2\pi^2 g(0) d^3$, where d is the diameter of the wire. Using these formulas, we estimated that for nanowires E1 and B2 at temperature $T = 0.4$ K, the predicted height of anomaly is $h_A \approx 0.014$, six times smaller than the experimental value. We conclude then that this theory also does not provide an adequate description of the anomaly in Mo-Ge nanowires.

In a previous section, we showed that the electron heating gives the correct estimate of the width of the ZBA in long *a*-$Mo_{50}Ge_{50}$ nanowires. Moreover, as Fig. 4(b) shows, the electron-phonon scattering length also appears to be a boundary separating the behavior of long and short nanowires. It is then natural to assume that electron heating is also responsible for the ZBA in our 150-nm-long nanowires. The details, however, should be different since, in short nanowires, most electrons leave the nanowire without a chance to experience an electron-phonon collision and thermalize. On the other hand, our estimates show that the length of the nanowires is somewhat larger than the electron-electron scattering length so, as a first approximation, we can adopt the picture that the electrons are thermalized amongst themselves and the electron temperature is well defined. The electrons and the lattice are then decoupled and the Joule heat generated in the wire is transferred to electrodes by diffusion. If we assume that the electron temperature is equal to the lattice temperature, T_{ph}, at the interconnection of the wire and the electrodes, the electron temperature as a function of the coordinate along the wire is given by the equation[57].

$$T(x) = \left(T_{ph}^2 + \frac{3}{\pi^2 L^2} x(L-x)\left(eV / k_B\right)^2 \right)^{1/2} \tag{4}$$

Using this equation, we find that when $T_{ph} = 0.4$ K and $V = 0.1$ mV (corresponding to the mid-height of the ZBA in Fig. 5c), the temperature in the middle of the wire is enhanced by $\Delta T \approx 0.11$ K. A larger temperature increase, $\Delta T \approx 0.4$ K, is needed to explain the drop of ZBA. We can suggest two additional processes enhancing the electron temperature. First, we notice that Eq. 4 was derived for the case when $T(0) = T(L) = T_{ph}$; experimentally this is achieved by covering electrodes with thick copper pads[58]. In our

structure, the electrodes are made of thin superconducting film and have small lateral extension (150 nm) in the immediate proximity of the nanowire. These factors suppress heat transfer and lead to an increase (perhaps significant) of $T(0)$ and $T(L)$ compared to T_{ph}. The second factor is that length of our wire is in the range $L_{\varphi} < L \cong L_{ee}$, so perhaps the electrons do not reach local equilibrium and are better described by the double-step Fermi distribution of the type observed in 1.5-μm-long copper wire in Ref. [60]. Then, assuming zero base temperature, at bias voltage $V_b = 0.1$ mV the effective temperature of the hot electrons in the middle of the wire would be $T_h = eV_b / 2k_B \approx 0.6$ K, which is high enough to provide required suppression of resistance. Our estimates thus show that the hot electrons are the cause of the ZBA in short nanowires. At the same time, because the length of our wires is not in the limiting cases easily described theoretically, a more complicated model including the propagation of heat in the electrodes is needed to give an accurate description of the phenomenon. An agreement with the theory of the weak Coulomb blockade appears to be accidental.

4. Summary

In summary, we have studied the zero bias anomaly, which appears in the differential resistance of insulating Mo-Ge nanowires with the length in the range of 150 nm - 11 μm. Studies of the nanowire-based structures with a gate electrode, "adiabatic" electrodes, and electrodes of variable size allowed us to exclude the weak Coulomb blockade and the anomaly in the tunneling density of states as the causes of the ZBA. We also found that the model of electron heating consistently and quantitatively explains the parameters of the ZBA and their evolution with changing nanowire's length. Overall, our work also suggests that electron heating cannot be ignored in the scaling analysis of the superconductor-insulator transition in Mo-Ge nanowires and films.

Acknowledgment

Authors would like to thank D. Pesin and E. Mishchenko for useful discussion. The work was supported by NSF grants DMR 1611421 and DMR 0955484.

[1] D.B. Haviland, Y. Liu, and A.M. Goldman, Phys. Rev. Lett. **62**, 2180 (1989).
[2] A. T. Bollinger, G. Dubuis, J. Yoon, D. Pavuna, J. Misewich, and I. Božović, Nature **472,** 458 (2011).
[3] N. Reyren, S. Thiel, A. D. Caviglia, L. Fitting Kourkoutis, G. Hammerl, C. Richter, C. W. Schneider, T. Kopp, A.-S. Rüetschi, D. Jaccard, M. Gabay, D. A. Muller, J.-M. Triscone, and J. Mannhar, Science **317**, 1196 (2007).
[4] N. Markovic, C. Christiansen, A.M. Mack, W.H. Hubner, and A.M. Goldman, Phys. Rev. B **60**, 4320 (1999).
[5] A. Yazdani and A. Kapitulnik, Phys. Rev. Lett. **74**, 3037 (1995).
[6] X. Leng, J. Garcia-Barriocanal, S. Bose, Y. Lee, and A.M. Goldman, Phys. Rev. Lett. **107**, 027001 (2012).
[7] H. Kim, S. Jamali, and A. Rogachev, Phys. Rev. Lett. **109**, 027002 (2012).
[8] Wei Ning, Hongyan Yu, Yequn Liu, Yuyan Han, Ning Wang, Jiyong Yang, Haifeng Du, Changjin Zhang, Zhiqiang Mao, Ying Liu, Mingliang Tian, and Yuheng Zhang, NanoLetters **15**, 869 (2015).
[9] N. Giordano, Phys. Rev. B **41**, 6350 (1990).
[10] F. Altomare, A. M. Chang, M.R. Melloch, Y. Hong, and C. W. Tu, Phys. Rev. Lett. 97, 017001 (2006).
[11] Ke Xu and J.R. Heath, NanoLetters **8**, 136 (2008).
[12] J.S. Lehtinen, T. Sajavaara, K. Yu. Arutyunov, M. Yu. Presnjakov, and A. L. Vasiliev, Phys. Rev. B **85**, 094508 (2012).
[13] M. Zgirski, K.-P. Riikonen, V. Touboltsev, and K. Arutyunov, Nanoletters, **5** ,1029 (2005).
[14] D.S Golubev, A.D. Zaikin, *Phys. Rev. B*, **64**, 014504 (2001).
[15] A. Bezryadin, *Superconductivity in nanowires. Fabrication and Quantum transport* (Wiley-VCH, Weinheim, 2013)
[16] M. Ovadia, D. Kalok, B. Sacépé, and D. Shahar, Nat. Phys. **9**, 415 (2013).

[17] C. Carbillet, S. Caprara, M. Grilli, C. Brun, T. Cren, F. Debontridder, B. Vignolle, W. Tabis, D. Demaille, L. Largeau, K. Ilin, M. Siegel, D. Roditchev, and B. Leridon, Phys. Rev. B **93**, 144509 (2016)
[18] K. A. Parendo, K. H. Sarwa, B. Tan, and A. M. Goldman, Phys. Rev. B 74, 134517 (2006)
[19] B. L. Altshuler and A. G. Aronov, in *Electron-Electron Interaction in Disordered Systems*, edited by A. L. Efros and M. Pollak (Elseveir Science Publ., Amsterdam, 1985).
[20] M. Bockrath, D.H. Cobden, J. Lu, A.G. Rinzler, R.E. Smalley, L. Balents, and P.L. McEuen, Nature **387**, 598 (1999).
[21] D. Goldhaber-Gordon, H. Shtrikman,D. Mahalu,D. Abusch-Magder,U. Meirav, M. A. Kastner, Nature **391**, 156 (1998).
[22] D. C. Ralph, A. W. W. Ludwig, Jan von Delft, and R. A. Buhrman, Phys. Rev. Lett. 72, 1064 (1994).
[23] R. M. Potok, I. G. Rau, H. Shtrikman, Yuval Oreg, D. Goldhaber-Gordon, Nature **446**, 167 (2007).
[24] W. Zheng, J.R. Friedman, D.V. Averin, S. Han, and J.E. Lukens, Solid State Comm. **108**, 839 (1998).
[25] F. Pierre, H. Pothier, P. Joyez, Norman O. Birge, D. Esteve, and M. H. Devoret, Phys. Rev. Lett. **86**, 1590 (2001).
[26] A. T. Bollinger, A. Rogachev, and A. Bezryadin, Europhys. Lett. **75,** 505 (2006).
[27] H.B. Weber, R. Haussler, H. v. Lohneysen, and J. Kroha, Phys. Rev. B, **63,**165426 (2001).
[28] D. Beckmann, H.B. Weber, and H. v. Lohneysen, Phys. Rev. B **70,** 033407 (2004).
[29] V.N. Bogomolov, E.V. Kolla, Yu.A. Kumserov, Solid State Commun, **43**, 156 (1983).
[30] D. N. Davydov, J. Haruyama, D. Routkevitch, B. W. Statt, D. Ellis, M. Moskovits, and J. M. Xu, Phys. Rev. B **57**, 13550 (1998).
[31] materials.springer.com
[32] D. Mael, S. Yoshizumi, and T.H. Geballe, Phys. Rev. B **34**, 467 (1986).
[33] H. Michor, T. Holubar, C. Dusek, and G. Hilscher, Phys. Rev. **B** 52, 16165 (1995); G.S. Knapp and R.W. Jones, Phys. Rev. **B 6**, 1761 (1972); Z. Lin, L.V. Zhigilei, and V. Celli, Phys. Rev. **B** 77, 075133 (2008).
[34] N.F. Mott, *Metal-Insulator Transition*, Taylor&Francis, London (2003).
[35] J. M. Graybeal, Ph.D. thesis, Stanford University 1985.
[36] U. Mizutani and T. Yoshida, J. Phys. F:Met. Phys., **10**, 2331 (1982).
[37]A. D. Zaikin, D. S. Golubev, A. van Otterlo, and G. T. Zimanyi, Phys. Rev. Lett. **78**, 1552 (1997).
[38] N. Giordano, Phys. Rev. B, 22, 5635 (1980).
[39] V. Chandrasekhar, Z. Ovadyahu, and R.A. Webb, Phys. Rev. Lett. 67, 2862 (1991).
[40] J.B. Kortright and A. Bienenstock, Phys. Rev. B **37**, 2979 (1988).
[41] M. J. Regan, M. Rice, M. B. Fernandez van Raap, and A. Bienenstock, Phys. Rev. Lett. **73**, 1118 (1994).
[42] M. J. Regan and A. Bienenstock, Phys.Rev. B **51**, 12170 (1995).
[43] Yu. V. Nazarov, Sov. Phys. JETP **68**, 561 (1989); JETP Lett. **49**, 126 (1989).
[44] M. H. Devoret, D. Esteve, H. Grabert, G.-L. Ingold, H. Pothier, and C. Urbina, Phys. Rev. Lett. **64**, 1824 (1990).
[45] P. Joyez, D. Esteve, and M. H. Devoret, Phys. Rev. Lett. **80**, 1956 (1998).
[46] Y.V. Nazarov, Phys. Rev. Lett. **82,** 1245 (1999).
[47] D.S. Golubev and A.D. Zaikin, Phys. Rev. Lett. **86,** 4887 (2001).
[48] J.T. Masden and N. Giordano, Phys. Rev. Lett. 49, 819 (1982).
[49] J.T. Masden and N. Giordano, Phys. Rev. B, 36, 4197 (1987).
[50] E.M. Gershenzon, M.E. Gershenzon, G.N. Go'tsman, A.M. Lyul'kin, A.D. Semenov, and A.V. Sergeev, Sov. Phys. JETP **70**, 505 (1990); R. Ceder, O. Agam, and Z. Ovadyahu, Phys. Rev B **72**, 245104 (2005).
[51] J. Liu, T.L. Meisenheimer, and N. Giordano, Phys. Rev. B 40, 7527 (1989)
[52] D.S. Golubev and A.D. Zaikin, Phys. Rev. Lett. **86,** 4887 (2001).
[53] J.P. Kauppinen and J.P. Pekola, Phys. Rev. Lett. **77,** 3889 (1996).
[54] P. Joyez. and D. Esteve, Phys. Rev. B **56,** 1848 (1997).
[55] J.P. Pekola, K.P. Hirvi, J.P. Kauppinen, and M.A. Paalanen, Phys. Rev. Lett. **73,** 2903(1994).
[56] D.S. Golubev and A.D. Zaikin, Phys. Rev. B, **70**, 165423 (2004).
[57] B. Huard, H. Pothier, D. Esteve, and K. E. Nagaev, Phys. Rev. B **76**, 165426 (2007).
[58] H. Pothier, S. Guéron, Norman O. Birge, D. Esteve, and M. H. Devoret, Phys. Rev. Lett. **79**, 3490 (1997).